

SIMULATION AND EXPERIMENTAL STUDIES ON WALKING ROBOT WITH FLEXIBLE LEGS

V. L. Krishnan^(a), P. M. Pathak^(b), Lokesh Sardana^(c), S. C. Jain^(d)

Robotics and Control Laboratory
Mechanical and Industrial Engineering Department
Indian Institute of Technology, Roorkee, 247667, India

^(a)vlk08dme@iitr.ernet.in, ^(b)pushpfme@iitr.ernet.in, ^(c)lokesume@iitr.ernet.in, ^(d)sjainfme@iitr.ernet.in

ABSTRACT

Passive motions caused by the elasticity of the muscles, tendons, and bones help animals in swimming, flying, breathing, running etc. This passive motion can be realized in artificial legged robots by using compliant elements viz. springs etc. Appropriate use of such elements can lead to power autonomous legged robots. Several attempts in exploiting compliance in legged robots are ongoing. Yet the scientific community is far from developing commercially viable flexible legged robots. In this work, simulation and experimental studies of sagittal plane dynamics of a flexible legged quadruped has been carried out. Bond graph is used as a tool for modeling and simulation of robot dynamics. Experimental studies have been carried out to explore the underlying principles and potential challenges in the locomotion of robots with flexible legs.

Keywords: legged robot, passive motion, flexible leg, sagittal plane, bond graph modeling.

1. INTRODUCTION

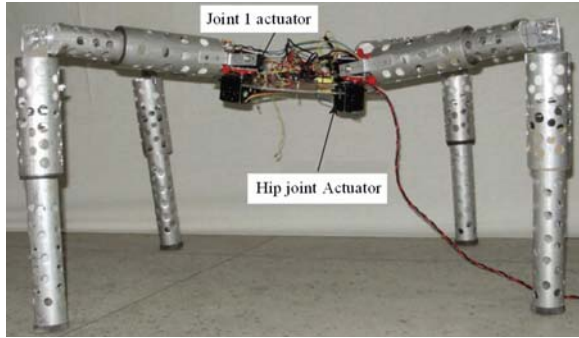
The most efficient way to create desired locomotion in case of legged robots is to generate it by the passive dynamic motion of a mechanism. Passive dynamics is defined as the unforced response of the dynamic system. Nature has gifted several animals the ability to exploit passive dynamics and thus to reduce the metabolic cost of running by utilizing the elastic properties of their muscles, tendons, and bones. Passive motions caused by the elasticity of the muscles, tendons, and bones help animals in swimming, flying, breathing, running etc. This passive motion can be realized in artificial legged robots by using compliant elements viz. springs etc. Compliant elements viz. different types of springs may be employed to realize coordinated oscillatory and translational motions of various parts of legged robots leading to various gaits viz. hopping, bounding, galloping etc. Appropriate use of such elements can lead to not only energy efficient but power autonomous legged robots. Raibert (1990) pioneered research pertaining to exploitation of passive dynamics for achieving dynamic legged locomotion. He achieved remarkable experimental success in realizing dynamic legged locomotion through his famous three-part controller. Buehler led a series of work (Ahmadi and Buehler 1997; Papadopoulos and Buehler 2000; McMordie and Buehler 2001) in this area leading to

development of multi-legged robots demonstrating stable, robust walking and running gaits. Hyon and Mita (2002) developed a single legged robot “Kenken”, similar to the hind leg of a dog in design, which successfully executed planar locomotion. They used springs and actuators to imitate tendons and muscles in the leg of a dog. Geyer, Seyfarth and Blickhan (2005) investigated the applicability of simple spring-mass models in analyzing the human and animal locomotion. Iida, Rummel and Seyfarth (2007) studied the role of compliance in bipedal walking and running behavior. Kimura, Fukuoka and Cohen (2007) employed central pattern generators to imitate neural system and reflex response of animals in the quadruped robot “Tekken” series. Zhang and Kimura (2009) further developed an autonomous running robot titled as ‘Rush’. However the research in this area is still continuing with the pursuit to develop commercially viable energy efficient (if not power autonomous) legged robots capable of performing stable locomotion at different speeds on various terrains.

In this work a flexible legged walking robot has been modeled by considering the sagittal plane representation of the quadruped robot locomotion. Bond graph is used as a tool for modeling and simulation of the robot dynamics. Robot dynamics in sagittal plane has been tested through the experiment. Experimental result shows the locomotion of the robot. Salient observations from the experiment are presented in this paper. The motive of the work is to use the passive component for force accommodation, and energy efficiency, as passive component can store energy in one step and release in other. Thus it saves the overall energy supplied to actuators.

2. MODELING OF WALKING ROBOT WITH FLEXIBLE LEGS

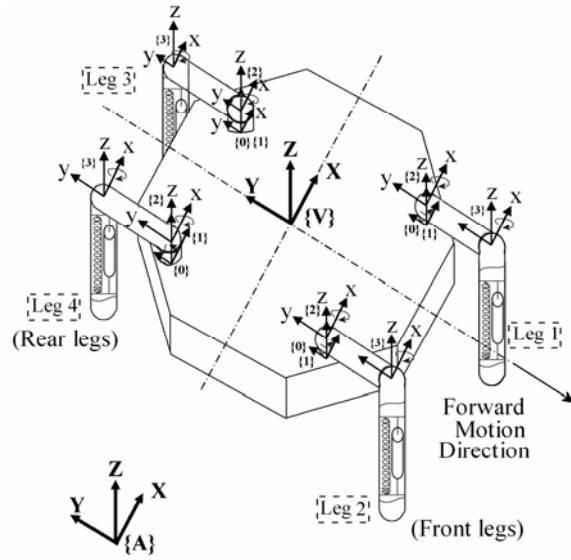
Modeling of a quadruped robot consists of modeling of translational and angular dynamics of robot legs and body. Figure 1(a) shows the laboratory prototype of the quadruped robot with flexible leg (Mittal, Lohani and Pandey 2009). The legs are made flexible using commercial shock absorber, shown in fig 1(b), in the lower link of the leg. Schematic diagram of the robot is shown in Fig. 1(c). Each leg of the robot has been modeled as an open chain manipulator comprising of two links connected through revolute joints. Thus each leg of the walking robot has three degrees of freedom



(a)



(b)



(c)

Fig. 1 (a) Quadruped Laboratory Prototype (b) Shock Absorber by ACE Controls Inc., MI, USA (c) Schematic Diagram of Flexible Legged Robot

and hence the robot has eighteen degrees of freedom (twelve degrees of freedom of legs and six degrees of freedom of body). The lower link mass of each leg is assumed to be concentrated at the leg toe. In the Fig. 1(c), frame $\{A\}$ is an inertial frame of reference and $\{V\}$ is body frame attached at the body CG. A coordinate frame is also attached to each link. The link frames are numbered according to the link to which

of motion of the robot has been chosen to be the negative Y -axis. The robot dynamics has been analyzed in the sagittal plane of locomotion i.e., YZ plane. It has been considered that the frontal dynamics can be taken care of with the help of an attitude control device viz. moving appendage employed in the transverse direction i.e. along X -axis. Moving appendage is an inertial element in the form of a rack to balance the disturbing moments on the body. The rack is driven through a pinion which in turn is actuated by a servomotor.

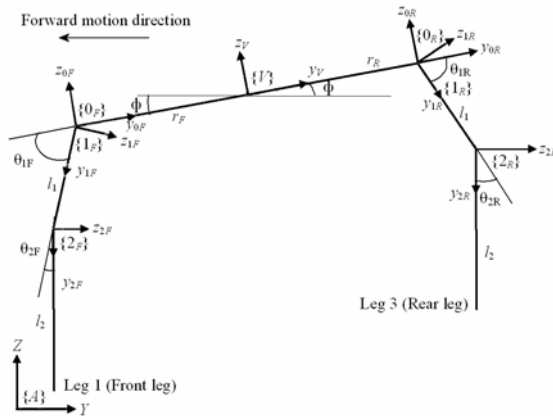


Fig. 2 Sagittal Plane Representation of Quadruped Robot

The corresponding representation of the kinematics of quadruped robot in the sagittal plane of locomotion is shown schematically in the Fig. 2. The figure shows the view of the robot with two degree of freedom (DOF) legs in a sagittal plane viz. YZ plane. The two DOF referred in fig 2. are in correspondence to joint 2 and 3 of a leg in fig. 1(c). The DOF at the hip joint of each leg (rotation about z axis), i.e. joint 1 in fig. 1 (c) is non-functional with respect to the current analysis and hence considered to be locked. From Fig. 2, the position of the front leg tip can be expressed in y and z -directions as,

$$Y_{Fi} = Y_{CM} + r_f \cos(\pi + \phi) + l_1 \cos(\pi + \phi + \theta_{1F}) + l_2 \cos(\pi + \phi + \theta_{1F} + \theta_{2F}) \quad (1)$$

$$Z_{Fi} = Z_{CM} + r_f \sin(\pi + \phi) + l_1 \sin(\pi + \phi + \theta_{1F}) + l_2 \sin(\pi + \phi + \theta_{1F} + \theta_{2F}) \quad (2)$$

they are attached i.e. frame $\{i\}$ is rigidly attached to link i . The joint between links i and $i+1$ is numbered as $i+1$. The rotational inertia of a body (or link) is defined about a frame fixed at the centre of gravity (CG) of the body (or link). The axis of the CG frame is fixed along the principal directions of the body (or link). The surface on which robot is walking is assumed as a hard surface with no slipping of legs. The forward direction

In Eq. (1) and (2) Y_{CM} and Z_{CM} represents the location of frame $\{V\}$ with respect to frame $\{A\}$; r_f is the distance of $\{0F\}$ frame from $\{V\}$ frame, ϕ is attitude of body with respect to frame $\{A\}$, θ_{1F} and θ_{2F} are the joint

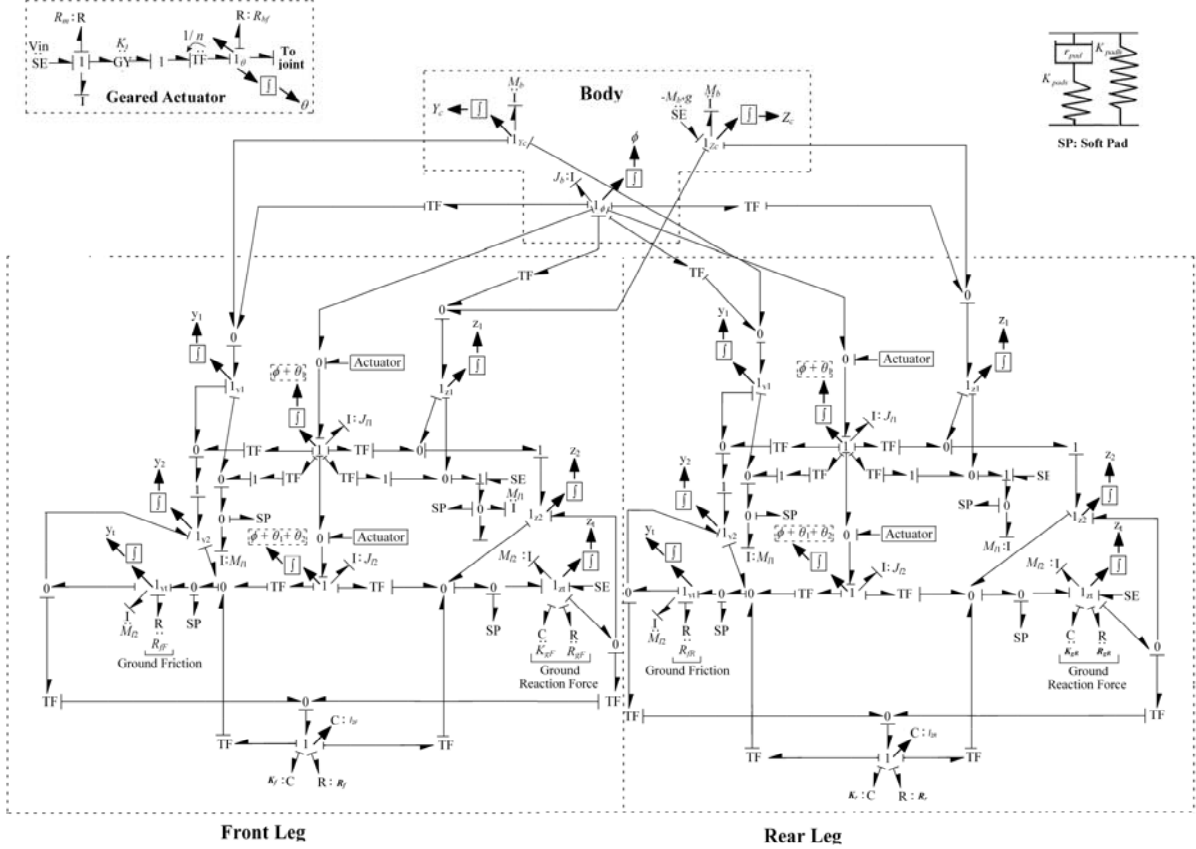


Fig. 3 Bond Graph representation of Sagittal Plane Dynamics of Flexible Legged Robot

angles of first and second joint of front leg, l_1 and l_2 are the lengths of the first and second links of a leg. Differentiating the expressions in Eq. (1) and (2), we get components of the front leg tip velocity in y and z-directions as,

$$\begin{aligned}
 V_{FY} &= \dot{Y}_{CM} - r_F \sin(\pi + \phi) \dot{\phi} \\
 &- l_1 \sin(\pi + \phi + \theta_{1F}) (\dot{\phi} + \dot{\theta}_{1F}) \\
 &- l_2 \sin(\pi + \phi + \theta_{1F} + \theta_{2F}) (\dot{\phi} + \dot{\theta}_{1F} + \dot{\theta}_{2F}) \\
 &+ \dot{l}_2 \cos(\pi + \phi + \theta_{1F} + \theta_{2F})
 \end{aligned} \quad (3)$$

$$\begin{aligned}
 V_{FIZ} &= \dot{Z}_{CM} + r_F \cos(\pi + \phi) \dot{\phi} \\
 &+ l_1 \cos(\pi + \phi + \theta_{1F}) (\dot{\phi} + \dot{\theta}_{1F}) \\
 &+ l_2 \cos(\pi + \phi + \theta_{1F} + \theta_{2F}) (\dot{\phi} + \dot{\theta}_{1F} + \dot{\theta}_{2F}) \\
 &+ \dot{l}_2 \sin(\pi + \phi + \theta_{1F} + \theta_{2F})
 \end{aligned} \quad (4)$$

Similarly, rear leg tip position with respect to inertial reference frame $\{A\}$ can be represented as,

$$\begin{aligned}
 Y_{Rt} &= Y_{CM} + (r_R \cos \phi) + l_1 \cos(\phi + \theta_{1R}) \\
 &+ l_2 \cos(\phi + \theta_{1R} + \theta_{2R})
 \end{aligned} \quad (5)$$

$$\begin{aligned}
 Z_{Rt} &= Z_{CM} + (r_R \sin \phi) + l_1 \sin(\phi + \theta_{1R}) \\
 &+ l_2 \sin(\phi + \theta_{1R} + \theta_{2R})
 \end{aligned} \quad (6)$$

Where r_R is the distance of frame $\{0_R\}$ from frame $\{V\}$, θ_{1R} and θ_{2R} are the joint angles of first and second joint of rear leg. It is assumed that initially rear leg link lengths are equal to the respective front leg link lengths. The rear leg tip velocities can be evaluated from Eq. (5) and (6) as,

$$\begin{aligned}
 V_{RY} &= \dot{Y}_{CM} - (r_R \sin \phi) \dot{\phi} - l_1 \sin(\phi + \theta_{1R}) (\dot{\phi} + \dot{\theta}_{1R}) \\
 &- l_2 \sin(\phi + \theta_{1R} + \theta_{2R}) (\dot{\phi} + \dot{\theta}_{1R} + \dot{\theta}_{2R}) \\
 &+ \dot{l}_2 \cos(\phi + \theta_{1R} + \theta_{2R})
 \end{aligned} \quad (7)$$

$$\begin{aligned}
 V_{RIZ} &= \dot{Z}_{CM} + (r_R \cos \phi) \dot{\phi} + l_1 \cos(\phi + \theta_{1R}) (\dot{\phi} + \dot{\theta}_{1R}) \\
 &+ l_2 \cos(\phi + \theta_{1R} + \theta_{2R}) (\dot{\phi} + \dot{\theta}_{1R} + \dot{\theta}_{2R}) \\
 &+ \dot{l}_2 \sin(\phi + \theta_{1R} + \theta_{2R})
 \end{aligned} \quad (8)$$

The flexibility of lower links of each leg is modeled on the basis of the following equations.

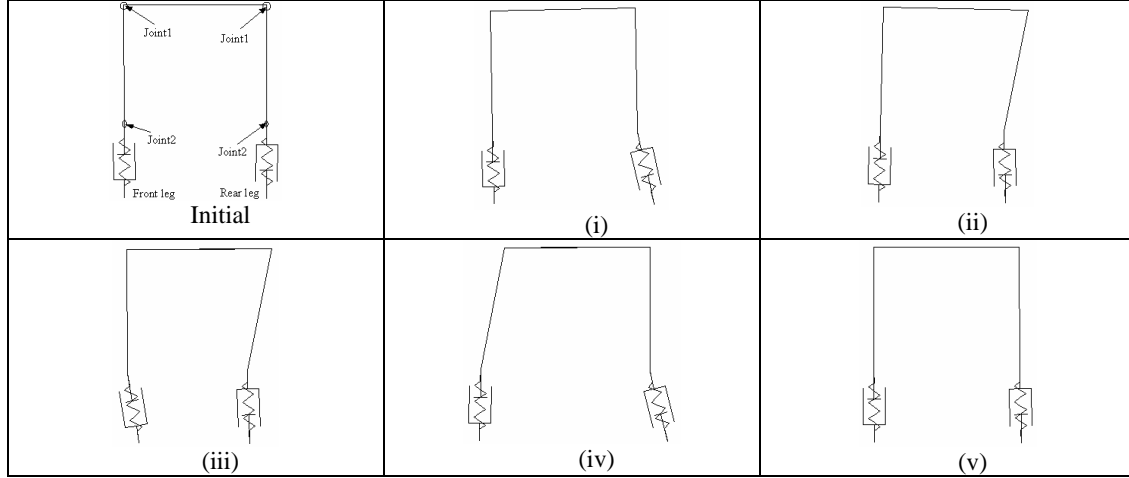


Fig. 4 Phases of gait pattern

$$(l_{2F})^2 = (Y_{Fl} - y_{2F})^2 + (Z_{Fl} - z_{2F})^2 \quad (9)$$

$$(l_{2R})^2 = (Y_{Rl} - y_{2R})^2 + (Z_{Rl} - z_{2R})^2 \quad (10)$$

where l_{2F} and l_{2R} are respectively the instantaneous lengths of link 2 of the front and rear legs. Y_{Fl} and Z_{Fl} are respectively the Y and Z coordinates of the toe of front leg and Y_{Rl} and Z_{Rl} of the rear leg.

Taking derivative of Eq. (9) and (10), we obtain respectively Eq. (11) and (12) as below:

$$\begin{aligned} (\dot{l}_{2F}) &= \frac{(Y_{Fl} - y_{2F})}{l_{2F}} * (\dot{Y}_{Fl} - \dot{y}_{2F}) \\ &+ \frac{(Z_{Fl} - z_{2F})}{l_{2F}} * (\dot{Z}_{Fl} - \dot{z}_{2F}) \end{aligned} \quad (11)$$

$$\begin{aligned} (\dot{l}_{2R}) &= \frac{(Y_{Rl} - y_{2R})}{l_{2R}} * (\dot{Y}_{Rl} - \dot{y}_{2R}) \\ &+ \frac{(Z_{Rl} - z_{2R})}{l_{2R}} * (\dot{Z}_{Rl} - \dot{z}_{2R}) \end{aligned} \quad (12)$$

With the help of Eq. (3), (4), (7), (8), (11) and (12) bond graph model is drawn in Fig. 3. It represents the sagittal plane dynamics of a quadruped robot with flexible legs. Further, in order that the robot demonstrates locomotion in the forward direction a gait pattern has been specified. The gait pattern is presented pictorially through fig. 4. The following steps describe the gait pattern:

1. Joint 2 of the rear leg (Leg3) to be rotated by 0.2 radians in *anticlockwise* direction about -x axis.
2. Joint 1 of the rear leg to be rotated by 0.2 radians in *clockwise* direction about -x axis.
3. Joint 2 of the front leg (Leg1) rotated by 0.2 radians in *anticlockwise* direction about -x axis.

4. Joint 1 of the front and rear legs are rotated by 0.2 radians respectively in *clockwise* and *anticlockwise* direction about -x axis.
5. Joint 1 of the front leg is rotated by 0.2 radians in *anticlockwise* direction and joint 2 of the front and rear legs are rotated by 0.2 radians in *clockwise* direction about -x axis.

Table1: Walking Robot Parameters

Parameters	Value
Walking robot Body	Mass: $M_b = 0.26\text{Kg}$; Polar M. I.: $J_b = 0.002\text{Kg-m}^2$
Position of Hip joints from body CG	Front: $r_F = 0.04\text{m}$; Rear: $r_R = 0.04\text{m}$
Link Lengths	$l_1 = 0.068\text{m}$, $l_2 = 0.04\text{m}$
Link Mass	$M_{l1} = 0.07\text{Kg}$; $M_{l2} = 0.06\text{Kg}$
Polar M. I of links	$J_{l1} = 0.00004\text{Kg-m}^2$; $J_{l2} = 0.00002\text{Kg-m}^2$
Actuator parameters	Inductance: $L_m = 0.001\text{H}$; Resistance: $R_m = 1000\text{Ohms}$; Motor constant: $K_t = 0.2\text{N-m/A}$; Gear Ratio: $n = 254$; Bearing resistance: $R_{bf} = 0.1\text{N-s/m}$
Ground Parameters	Stiffness: $K_g = 10000\text{N/m}$; Damping: $R_g = 10\text{N-s/m}$; frictional resistance: $R_{\gamma} = 10\text{N-s/m}$
Flexible Link parameters	Stiffness: $K_f = 350\text{N/m}$; Damping $R_f = 0.35\text{N-s/m}$

The above steps of a gait together forms a locomotion cycle. This gait is repeated over ten cycles to

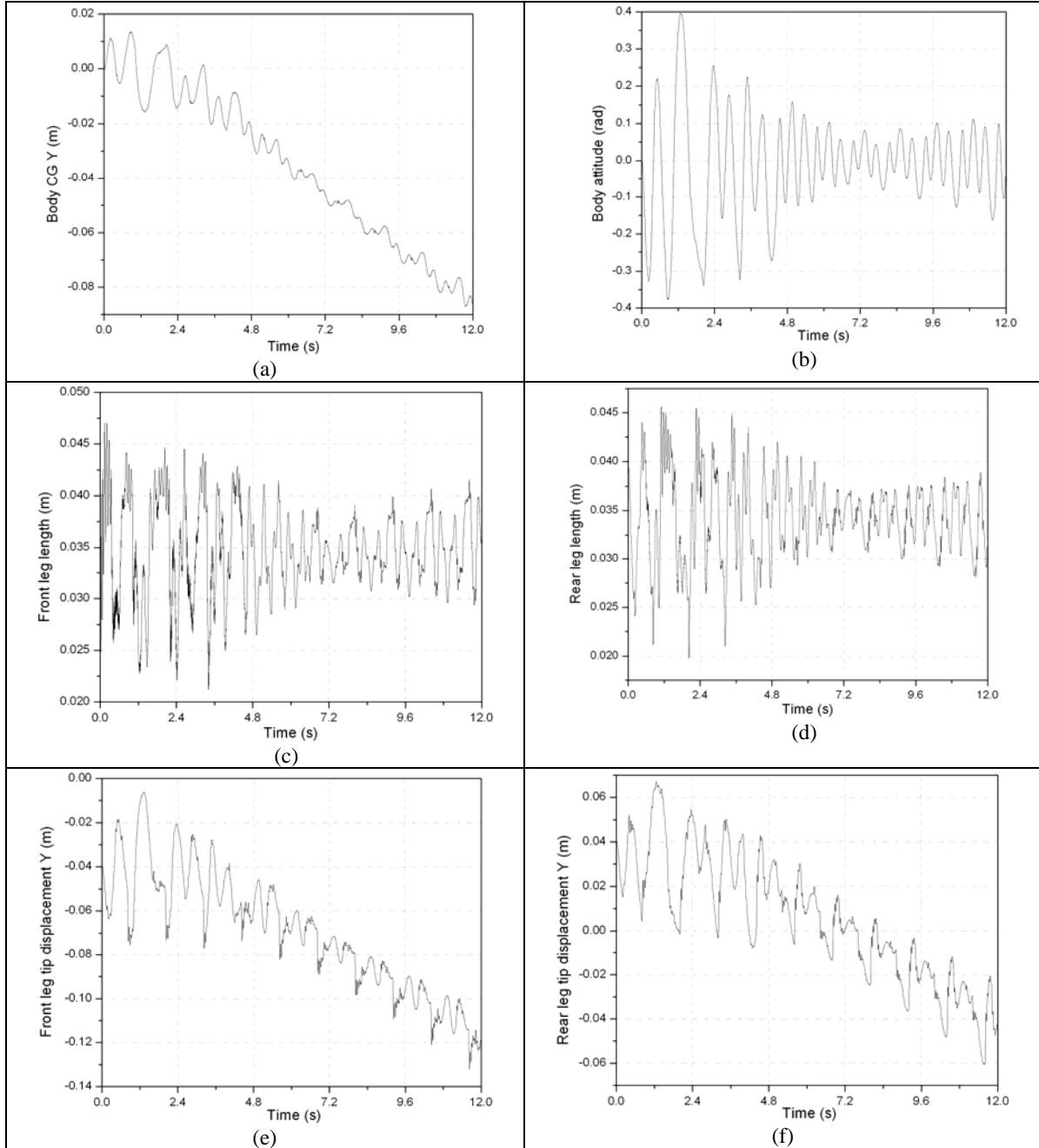


Fig. 5 Simulation results of sagittal plane locomotion of flexible legged robot (a) Body CG Y displacement v/s time (b) Body attitude v/s time (c) Front Leg Length v/s time (d) Rear Leg Length v/s time (e) Front leg tip displacement v/s time (f) Rear leg tip displacement v/s time

demonstrate the body advancement in the forward direction. To take the joint angles to the specified value of joint angles the voltage supplied to motor is based on PD control. One locomotion cycle is assumed to be of 1.2 seconds. The parameters used for simulation are listed in table 1.

Fig. 5 shows the simulation results of sagittal plane locomotion of flexible legged robot over a period of 12s. Fig. 5 (a) shows the body CG Y displacement versus time. It can be noted that the body displacement

in -Y direction occurs. Fig. 5 (b) presents the body attitude versus time. Fig. 5(c) shows the variation of instantaneous length of lower link of front leg i.e. l_{2F} versus time. Similarly Fig. 5 (d) shows the variation of l_{2R} versus time. The results indicate the flexibility modeled in the lower link of each leg. Fig. 5 (e) shows the front leg tip displacement versus time. Fig. 5 (f) shows the rear leg tip displacement versus time. These figures show the locomotion of the robot with flexible legs. Fig. 6(a) shows the front leg joint '1' angle

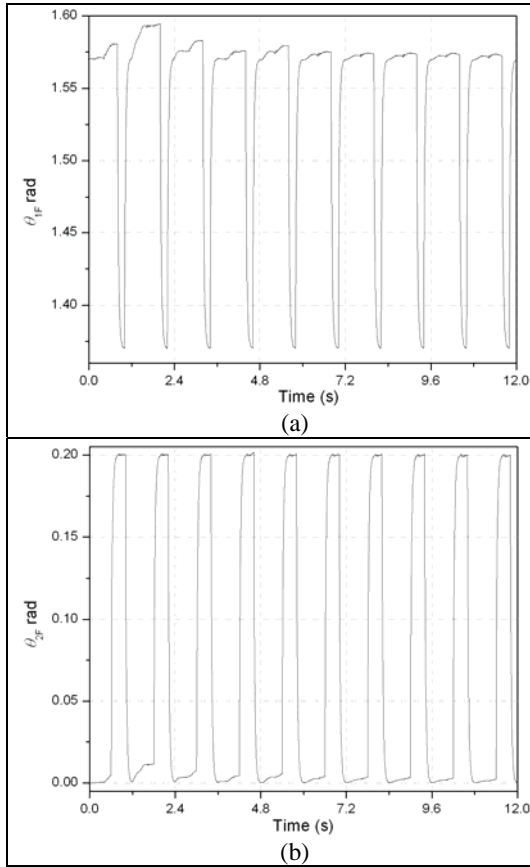


Fig. 6 Simulation results (a) θ_1 Front leg v/s time (b) θ_2 Front leg v/s time

displacement versus time. Fig. 6(b) presents the front leg joint '2' angle displacement versus time. Rear leg joint '1' angle displacement versus time is shown in fig. 6(c). Fig. 6(d) presents the rear leg joint '2' angle displacement versus time. Fig. 7 shows the animation result which indicates desired forward motion of the walking robot. Animation has been generated from the simulation results. Here only few frames are shown to have clarity in the figure.

3. EXPERIMENTAL RESULTS

The sagittal plane dynamics of walking robot has been tested through the experimental set up shown in fig. 8. The experimental setup comprises of a post which supports the planar model of the flexible legged quadruped robot through a horizontal rod. The body of the robot is pivoted about the rod. Thus it is constrained to move along a circular trajectory about the post. Hence, the instantaneous response of robot is restricted to a plane tangential to the circular trajectory. In this way the sagittal plane response of the robot is realized. The planar model of flexible legged robot consists of body, legs and actuators at the two joints in each of the front and rear legs. Hence, in total four AX-12+ motors (Dynamixel make) are used to realize the two link legs. The controller CM5+ housed in a plastic sturdy shell

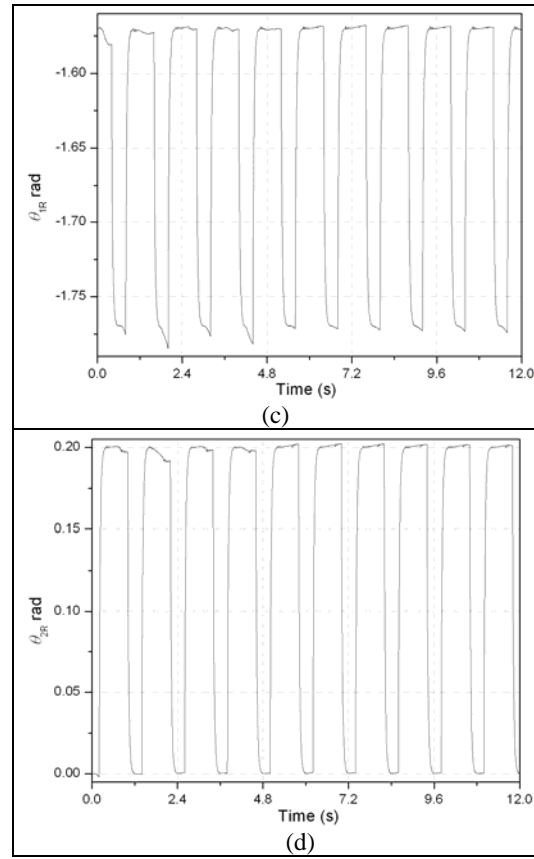


Fig. 6 Simulation results (c) θ_1 Rear leg v/s time (d) θ_2 Rear leg v/s time

constitutes the body of the robot. Springs are attached to the lower link of each leg to introduce flexibility into the legs.

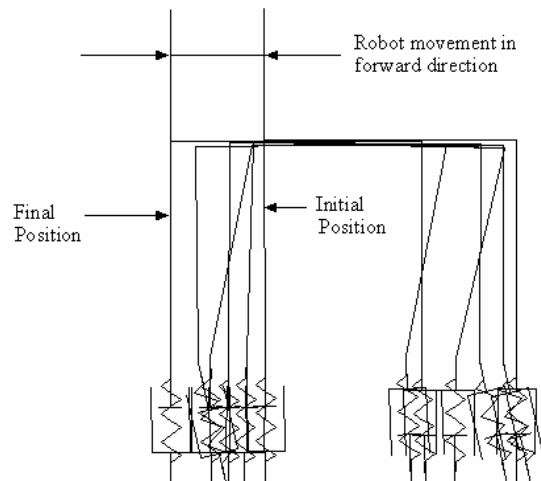


Fig. 7: Animation of Walking Robot Motion

The flow chart corresponding to the gait pattern used for the robot locomotion control is presented in fig. 9. Bioloid control behavior interface of the Robotis

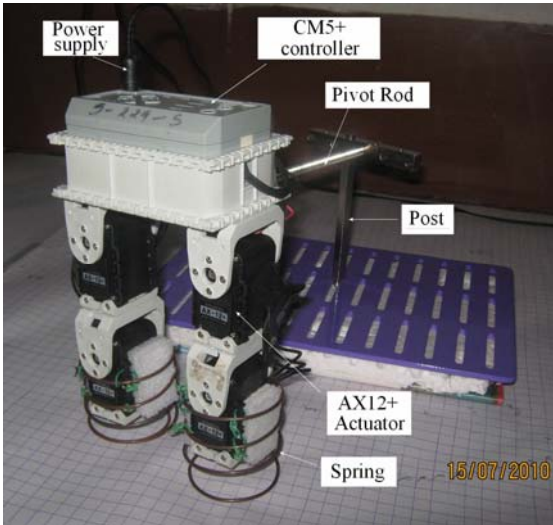


Fig.8: Experimental set up representing saggital plane dynamics of walking robot

Inc. is used for the purpose of controlling robot locomotion. The program is fed to the CM5+ controller through personal computer (not shown in the fig. 8). SMPS is used for supplying required power to the actuators and electronic circuitry.

Fig. 10 presents the snapshots of robot locomotion. It can be noted from the snapshots that the robot is constrained, through the pivot rod connected to post, to trace a semicircular trajectory. Fig. 11 shows the actual joint angle displacement of legs. Fig. 11(a) and (b) respectively shows the front leg first and second joint rotation versus time. Fig. 12(a) and (b) respectively shows the rear leg first and second joint rotation versus time. It can be noted from the plots of joint rotation curves that the specified gait pattern is being followed. The joint rotation curves in fig. 11 and 12 are similar to the simulated results in fig. 6. Fig. 13 presents the front and rear leg tip movement versus time, recorded over first ten locomotion cycles. Front and rear leg tip movement pattern is similar to simulated results presented in Fig. 5(e) and 5(f). It can be noted that simulation is also carried out for ten locomotion cycles i.e for 12 seconds. The leg tip movement values plotted in fig 13 is the arc length translated by the leg tip along a semicircular trajectory versus time. It can be noted that the arc length traced at the end of ten cycles by the front and rear leg tips are respectively about 0.16m and -0.04m which is very close to corresponding simulation results. Thus the robot locomotion in forward direction based on the specified gait pattern is obtained.

4. CONCLUSION AND DISCUSSIONS

Following observations has been made while realizing the saggital plane locomotion of the robot:

- (i) Stiffness of the spring selected should be appropriate. It should be within an optimum range so that it absorbs undesirable impact

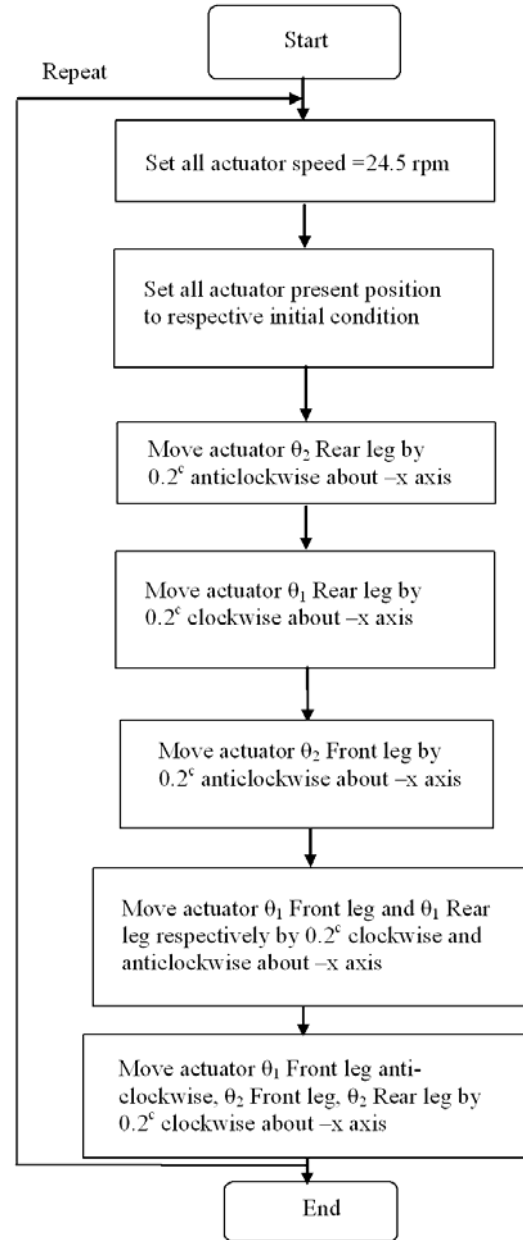


Fig. 9: Flowchart of the program for locomotion control

forces coming from the ground while in locomotion. At the same time less stiffer springs will not generate traction force required for locomotion.

- (ii) The clearance between the springs and the leg links should be minimum possible so that the link rotation may carry the spring also along with it.

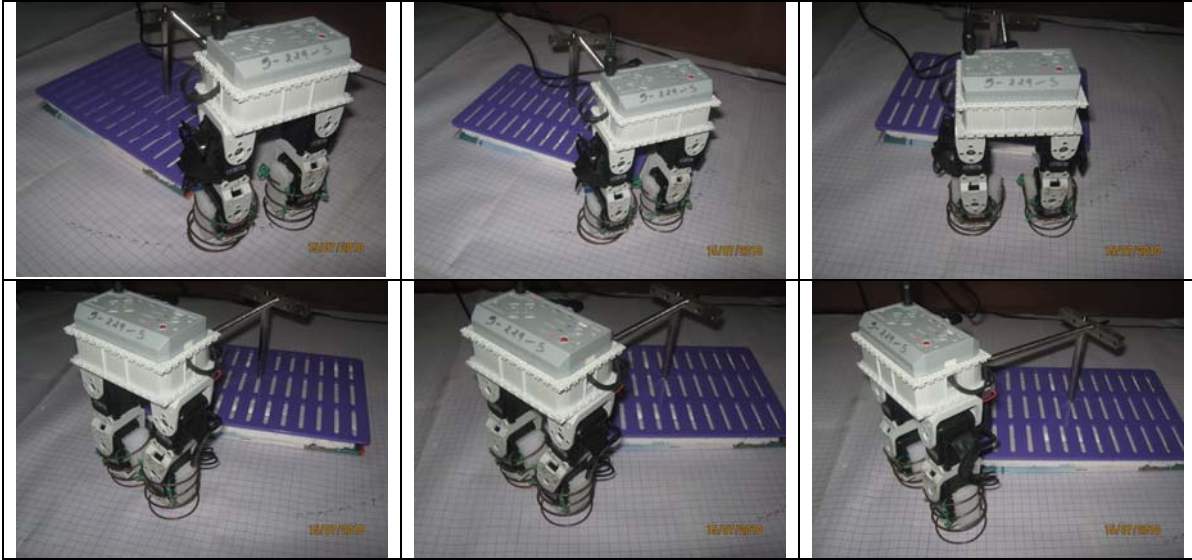


Fig. 10 Snapshots of sagittal plane locomotion of flexible legged walking robot

(iii) There can be alternative gait patterns leading to faster and stable locomotion which is a matter of further investigation.

In the present experimental setup provision for recording the ground reaction forces and the traction force does not exist. In future, force sensors can be employed at the toe and investigations pertaining to the

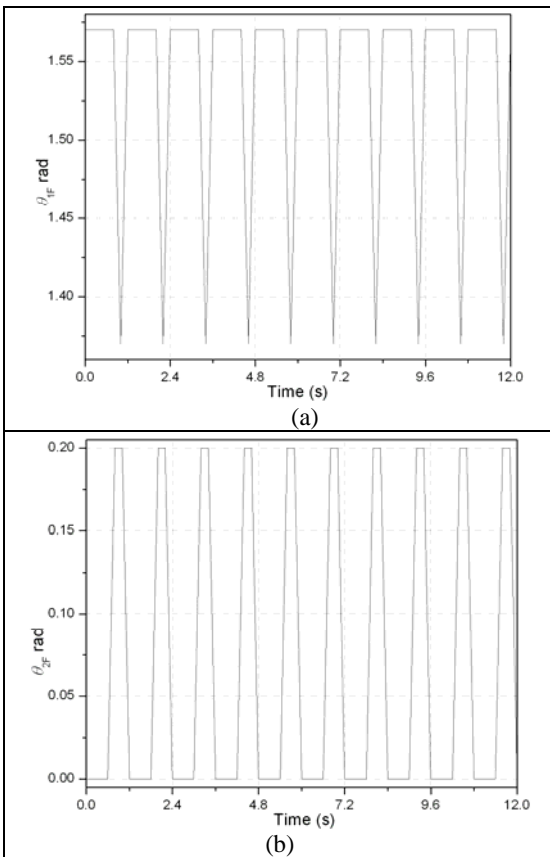


Fig. 11 Joint rotation for Front leg obtained from Experiment (a) θ_1 v/s time (b) θ_2 v/s time

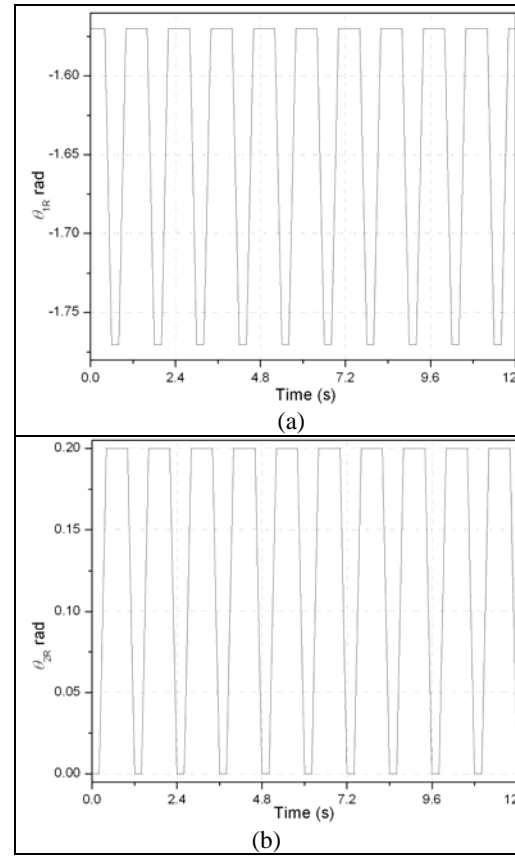


Fig. 12 Joint rotation for Rear leg obtained from Experiment (a) θ_1 v/s time (b) θ_2 v/s time

role of passive elements viz. spring in absorbing impact forces can be carried out. The ultimate aim is to implement the force control strategy with the help of flexible link and to extend the developed strategy to four legged walking robot with flexible legs.

(ii) In future the present setup is proposed to be used for studies aiming at improving the energy efficiency of the robot locomotion.

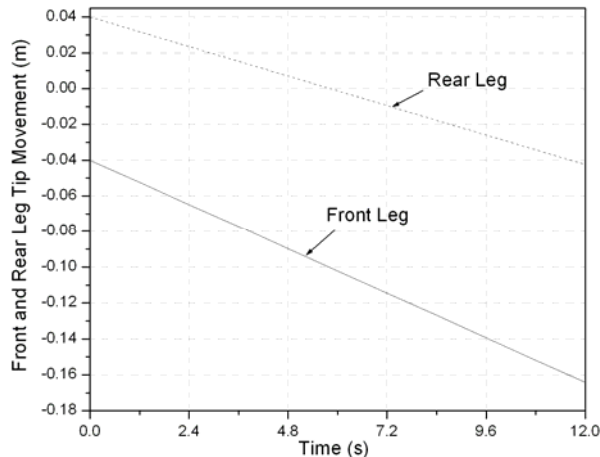


Fig. 13: Front and Rear Leg Tip Forward Movement (m) v/s time (s)

REFERENCES

- Ahmadi, M. and Buehler, M., 1997, Stable Control of a Simulated One-Legged Running Robot with Hip and Leg Compliance, *IEEE Transactions on Robotics and Automation*, 13 (1); 96 – 104.
- Geyer, H., Seyfarth, A. and Blickhan, R., 2005, Spring-Mass Running: Simple Approximate Solution and Application to Gait Stability, *Journal of Theoretical Biology*, 232(3); 315-328.
- Hyon, S. H. and Mita, T., 2002, Development of a biologically inspired hopping robot: Kenken, *Proceedings of IEEE International Conference on Robotics and Automation*, Vol. 4, pp. 3984–3991, 11-15 May, Washington, DC (U.S.A).
- Iida, F., Rummel, J. and Seyfarth, A., 2007, Bipedal Walking and Running with Compliant Legs, *Proceedings of IEEE International Conference on Robotics and Automation*, pp. 3970–3975, 10-14 April., Roma, Italy.
- Kimura, H., Fukuoka, Y. and Cohen, A. H., 2007, Adaptive Dynamic Walking of a Quadruped Robot on Natural Ground based on Biological Concepts, *Int. Journal of Robotics Research*, 26(5); 475-490.
- McMordie, D. and Buehler, M., 2001, Towards Pronking with a Hexapod Robot, *Proceedings of 4th International Conference on Climbing and Walking Robots*, pp. 659-666, 24-26 September, Karlsruhe, Germany.

Mittal A., Lohani H. and Pandey A., 2009, *Dynamic Analysis of a Quadruped Robot*, B. Tech thesis, IIT Roorkee, Roorkee, India.

Papadopoulos, D. and Buehler, M., 2000, Stable Running in a Quadruped Robot with Compliant Legs, *Proceedings of IEEE International Conference on Robotics and Automation*, Vol. 1, pp. 444–449, 24-28 April, San Francisco (U.S.A).

Raibert, M. H., 1990, Trotting, Pacing and Bounding by a Quadruped Robot, *Journal of Biomechanics*, 23(1); 79-81.

Zhang, Z. G. and Kimura, H., 2009, Rush: A Simple and Autonomous Quadruped Running Robot, *Journal of Systems and Control Engineering*, 223(1), 323-336.

